Volume 22, No 3 | International Journal of Radiation Research, July 2024

Using conventional contrast-enhanced MRI semi-quantitative analysis to distinguish alpha-fetoprotein-negative small hepatocellular carcinoma without cirrhosis and small focal nodular hyperplasia

X. Zhu[1,2], Q. Feng[1,2], X. Ge[1,2*], B. Hu[3*]

[1]The Fourth Clinical College, Zhejiang Chinese Medical University, Hangzhou, 310000, P.R.China
[2]Department of Radiology, the Affiliated Hangzhou First People's Hospital, Zhejiang University School of Medicine, Hangzhou, Zhejiang, China
[3]Department of Radiology, ChunAn County First People's Hospital, Zhejiang, China

► ***Original article***

Corresponding author:
Xiuhong Ge & Bo Hu,
E-mail:*478556386@qq.com, 570396920@qq.com*

Received: January 2023
Final revised: February 2024
Accepted: February 2024

Int. J. Radiat. Res., July 2024; 22(3): 625-630

DOI: 10.61186/ijrr.22.3.625

Keywords: *Gray scale value; MRI; semi-quantitative analysis; liver cancer, hepatocytes; focal nodular hyperplasia; quantitative analysis.*

ABSTRACT

Background: Here, we aimed to quantitatively analyze the gray scale value (GSV) of conventional triple-enhancement MRI and explore its value in differentiating non-cirrhosis, alpha-fetoprotein-negative small Hepatocellular carcinoma (SHCC) together with Focal nodular hyperplasia (SFNH). ***Materials and Methods:*** In this study, 83 cases of SHCC-related lesions were observed in 83 individuals, and an additional 35 cases of SFNH-associated lesions were examined in a group of 32 patients. These lesions were all verified through pathological assessment. The lesions' MRI GSV of the plain scan (GSV-p) and the enhanced MRI scan (GSV-c), and normal liver parenchyma's GSV around the lesion (GSV-n) were all quantified. Subsequently, we computed the GSV-c to GSV-n ratio (GSR), and the GSV-c to GSV-p ratio (GSRL). We employed the Wilcoxon rank sum analysis and ROC curve analysis with the aim of evaluating significance in these ratios. ***Results:*** Age and gender distribution in SHCC and SFNH exhibited relevant differences, whereas the size did not. During the phases arterial (GSRAP), portal (GSRPP), and delayed (GSRDP), the GSR and the GSRL for SHCC and SFNH demonstrated a gradual decrease, and all these changes were statistically significant. The AUC for GSRDP in SHCC and SFNH was 0.83, which surpassed the performance of other metrics. ***Conclusions:*** The GSV values obtained from a standard triple-enhancement MRI were found to be valuable in distinguishing between SHCC and SFNH, with the GSRDP showing the best performance. The precise utilization of these metrics facilitated the differentiation of SHCC and SFNH, ultimately reducing the need for unnecessary interventional procedures and associated trauma.

INTRODUCTION

Hepatocellular carcinoma (HCC) stands as the primary malignant liver tumor of highest prevalence, ranking as number two or three for mortality derived from cancerous diseases [1-3]. Focal nodular hyperplasia (FNH) ranks second in terms of benign nodular liver lesions [4,5]. Remarkably, both conditions exhibit heightened vascularity. HCC is distinctive for its rapid contrast agent clearance during the phases portal and delayed, distinguishing it from the neighboring liver tissue [6], whereas FNH exhibits iso-intensity or mild hyper-intensity in the venous phase, attributed to its slower washout dynamics [7].

Alpha-fetoprotein (AFP) has the function of a biomarker and helps diagnose HCC [3,8]. Raised levels of AFP in the blood and characteristic imaging features make it relatively easy to diagnose AFP-positive HCC. However, approximately 30% of individuals with HCC remain AFP-negative [3], and thus, diagnosing AFP-negative HCC (ANHC) becomes challenging due to the absence of ideal biomarkers, primarily relying on imaging [9]. The presence of fibrotic or cirrhotic livers is a relevant risk indicator for HCC, and liver fibrosis has a fundamental part in the premalignant environment (PME) of the liver [10]. Around twenty percent of HCC cases may originate cirrhosis-free context, referred to as non-cirrhotic HCC (NCHCC) [11-14]. Consequently, diagnosing NCHCC patients who are both AFP-negative and lack cirrhosis presents a complex challenge.

Specialized liver contrast agents, like gadoxetic acid, can furnish more precise diagnostic information for these conditions [15-17]. Nevertheless, the use of such agents can impose an added financial burden on patients and may potentially result in delayed diagnoses. At times, HCC and FNH can exhibit perplexing or atypical manifestations on imaging, particularly in the case of high- or middle-grade

[DOI: 10.61186/ijrr.22.3.625]

differentiated small HCC (SHCC), causing uncertainty and misdiagnosis [18]. It is critical to differentiate between these two conditions as their treatments differ [19,20]. In order to evade unnecessary invasive procedures or examinations like biopsies, surgical interventions, or medical therapies, which have a substantial effect on the prognosis and quality of life for individuals, it is crucial to establish an accurate non-invasive diagnosis before undergoing any surgical intervention.

In this study, standard enhanced magnetic resonance imaging (MRI) was employed alongside a semi-quantitative analysis approach to differentiate between SHCC (lacking cirrhosis and having negative AFP) and small FNH (SFNH, with a diameter not exceeding 3 cm). This approach potentially enhances diagnostic precision, offering potential advantages for clinical treatment and patient care.

MATERIALS AND METHODS

Approval for this research was granted by the Ethics Committee of Hangzhou First People's Hospital, which is associated with Zhejiang University School of Medicine, under reference number NO. 109 - 01. The study followed the guidelines set forth in the Declaration of Helsinki, and every subject involved furnished written informed consent.

Participants

This retrospective assessment focused on cases of SHCC and SFNH (diagnosis period length: January, 2014, to December, 2019). The enrolled subjects met the following criteria: 1) all individuals underwent a triple-enhancement MRI scan; 2) the maximum lesion diameter was less than 3 cm; 3) serum AFP levels were below 10 ng/mL; 4) absence of cirrhosis in all patients; and 5) confirmation of SHCC and SFNH diagnoses via immunohistochemical analysis. The exclusion criterion was the presence of fatty liver in patients [21]. A total of 83 HCC lesions in 83 patients (comprising 74 men and 9 women, ages 52 - 66) and 35 FNH lesions in 32 patients (consisting of 14 men and 18 women, ages: range 24 - 42) were analyzed.

MRI scanning procedure and parameters

All patients received imaging using a 3.0 Tesla MR scanner purchased from Sigma HDxt (GE Medical Systems) with a phased-array body coil. The imaging protocol encompassed three methods: The T1-weighted (T1WI), the axial T2-weighted (T2WI), and the diffusion-weighted (DWI). Subsequently, multi-phase T1WI dynamic-contrast-enhanced MRI scans were carried out. These comprised non-enhanced imaging and three post-enhancement phases at 15, 60, and 120 seconds after the provision of contrast agents based on gadolinium [22].

The MRI parameters were as follows: T2-weighted imaging (TR = 2500 ms; thickness, 6 mm; echo time = 80 ms; voxel magnitude = 1.5×1.5×6.0 mm^3; field of view = 380 × 308.94 mm^2; turning angle = 126 degrees) and T1-weighted image (TR = 3.92 ms; thickness, 3 mm; echo time = 1.30 ms; voxel size = 2.1 × 1.5 × 3.0 mm^3; field of view = 380 × 380 mm^2; turning angle = 9 degrees), followed by axial DWI (TR = 6800 ms; thickness, 5 mm; echo time = 70 ms; voxel size = 3.5 × 2.7 × 5.0 mm^3; field of view = 380 × 271.32 mm^2;) with b= 0 and 800 s/mm^2.

MRI imaging analysis

Two radiologists independently conducted a blind assessment of the MRI images. A circular or elliptical region of interest (ROI) with an area ranging from 15 to 35 mm^2 and uniform density within the lesion was chosen. Gray scale values (GSV) were recorded at the corresponding position within the lesion, ensuring exclusion of necrotic areas and vascular structures. The distance between the ROI in the adjoining healthy hepatic parenchyma and the lesion showed to be greater than 1.0 cm, and this methodology and size alignment adhered to the ROI of the lesion (figure 1) [22].

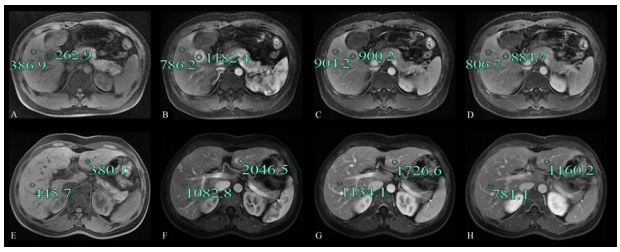

Figure 1. The diagram of delineate the ROI of the SHCC and SFNH. **A.B.C.D** representation the plain, AP, PP and DP of the SHCC respectively; **E.F.G.H** representation the plain, AP, PP and DP of the SFNH respectively. ROI: region of interest, SHCC: small Hepatocellular carcinoma, SFNH: small Focal nodular hyperplasia.

We quantified the MRI gray scale values (GSV) of the lesions in both the unenhanced scan (GSV-p) and the contrast-enhanced MRI scan (GSV-c), as well as the GSV of the normal liver parenchyma surrounding the lesion (GSV-n). Subsequently, we computed the GSV-c to GSV-n ratios (GSR) and the GSV-c to GSV-p ratios (GSRL) for the phases portal (PP), arterial (AP), and delayed (DP).

Statistical analysis

Statistical analyses of clinical variables were carried out utilizing SPSS software (version 22). Continuous variables, such as age and lesion size, appeared as mean ± standard deviation. Gender variances between groups underwent comparisons through the chi-square test. Diagnostic performance was evaluated through metrics including the area under the receiver operating curve (AUC), specificity, sensitivity, and accuracy. The Cohen kappa coefficient was employed to gauge how the two radiologists agreed in their resolution.

[DOI: 10.61186/ijrr.22.3.625]

RESULTS

Demographic and clinical data

This study comprised 83 HCC patients (74 women, 9 men) with a mean age of 58 (range: 52 - 66), as well as 32 FNH patients (14 women, 18 men) with a mean age of 29 (range: 24 to 42). Among the 83 HCC patients, there were a total of 83 SHCC lesions, while the 32 FNH patients presented a total of 35 FNH lesions. The FNH patients had varying lesion counts: 30 subjects had 30 lesions, 1 subject had 2, and 1 subject had 3. The size of SHCC lesions averaged 2.4 cm (range:1.8 to 2.8 cm), and SFNH lesions averaged 2.2 cm (range: 1.8 to 2.6 cm) (P = 0.172) (table 1).

Table 1. Clinical features of patients with SHCC or SFNH.

Characteristic	SHCC	SFNH	*P*
No. of nodules	83	35	NA
No. of patients	83	32	NA
Sex, no. of patients			0.001
Male	74	14	NA
Female	9	18	NA
Age (y), mean (range)	58(52~66)	29(24~42)	0.001
Size(cm) mean (range)	2.4 (1.8~2.8)	2.2 (1.8~2.6)	0.172

SHCC, small Hepatocellular carcinoma; SFNH, small focal nodular hyperplasia.

The GSR of AP, PP, and DP

The GSR values in the phases arterial (GSRAP), portal (GSRPP), and delayed (GSRDP) for SHCC and SFNH were as follows: 1.46 (ranging from 1.34 to 1.80) vs 1.92 (ranging from 1.67 to 1.80) (Z = -3.945, P < 0.01) for GSRAP, 0.95 (ranging from 0.87 to 1.03) vs. 1.11 (ranging from 1.01 to 1.19) (Z = -4.681, P < 0.01) for GSRPP, and 0.92 (ranging from 0.80 to 0.97) vs. 1.02 (ranging from 1.00 to 1.09) (Z = -5.624, P < 0.01) for GSRDP, respectively (table 2).

Table 2. The GSR and GSRL of the AP, PP, and DP of the SHCC and SFNH.

		GSR			GSRL		
		AP	PP	DP	AP	PP	DP
SHCC	83	1.46 (1.34~ 1.80)	0.95 (0.87~ 1.03)	0.92 (0.80~ 0.97)	2.55 (2.00~ 3.14)	2.32 (2.02~ 2.76)	1.92 (1.78~ 2.33)
SFNH	35	1.92 (1.67~ 2.18)	1.11 (1.01~ 1.19)	1.02 (1.00~ 1.09)	3.25 (2.60~ 3.85)	2.89 (2.36~ 3.16)	2.40 (1.98~ 2.68)
Z		-3.945	-4.681	-5.624	-3.921	-3.456	-1.365
P		0.001	0.001	0.001	0.001	0.001	0.001

GSR, MRI grayscale ratio between the lesion and the surrounding normal liver parenchyma; GSRL, MRI grayscale ratio between the enhance-lesion and the plain scan-lesion; SHCC, small Hepatocellular Carcinoma; SFNH, small Focal nodular hyperplasia; AP, arterial phase; PP, portal phase; DP, delayed phase.

The GSRL values in the phases arterial (GSRLAP), porta (GSRLPP), and delayed (GSRLDP) for SHCC and SFNH were as follows: 2.55 (ranging from 2.00 to 3.14) vs. 3.25 (ranging from 2.60 to 3.85) (Z = -3.921, P < 0.01) for GSRLAP, 2.32 (ranging from 2.02 to 2.76) vs. 2.89 (ranging from 2.36 to 3.16) (Z = -3.456, P < 0.01) for GSRLPP, and 1.92 (ranging from 1.78 to 2.33) vs. 2.40 (ranging from 1.98 to 2.68) (Z = -1.365, P < 0.01) for GSRLDP, respectively (see table 2).

Diagnostic Performances

The AUC values for GSRAP, GSRPP, and GSRDP in distinguishing SHCC from SFNH were 0.73, 0.77, and 0.83, respectively. The corresponding outcomes for sensitivity and specificity were 74.3% and 73.5%, 91.4% and 67.5%, 82.9% and 85.5%. The positive likelihood and negative likelihood ratios (+LR and -LR, correspondingly) were 2.80 and 0.35, 2.81 and 0.13, 5.72 and 0.20, respectively. The optimal threshold values for GSRs showed to be 1.70, 0.99, and 0.99, and the highest Youden indexes were 0.48, 0.59, and 0.68, correspondingly (figure 2, table 3).

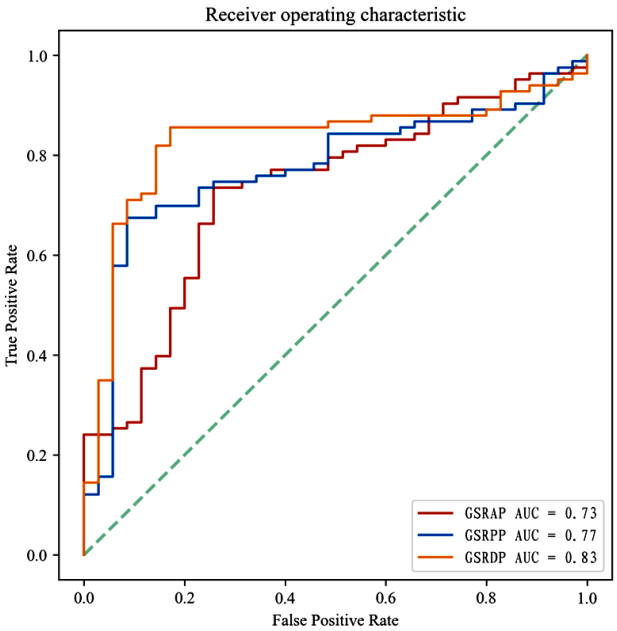

Figure 2. ROC curve generated according to GSRAP, GSRPP and GSRDP values. *ROC: receiver operating curve, GSR: MRI grayscale ratio between the lesion and the surrounding normal liver parenchyma, AP: arterial phase, PP: portal phase, DP: delayed phase, GSRAP: GSR in the AP, GSRPP: GSR in the PP, GSRDP: GSR in the DP.*

Table 3. The sensitivity, specificity, +LR, and -LR of GSR and GSRL of AP, PP and DP of SHCC and SFNH when the Youden index was maximum.

Phase	AUC	YD_{max}	Sen(%)	Spe (%)	+LR	-LR
GSRAP	0.73	0.48	74.3	73.5	2.80	0.35
GSRPP	0.77	0.59	91.4	67.5	2.81	0.13
GSRDP	0.83	0.68	82.9	85.5	5.72	0.20
GSRLAP	0.73	0.37	68.6	68.7	2.19	0.46
GSRLPP	0.70	0.38	51.4	86.7	3.86	0.56
GSRLDP	0.70	0.34	62.9	71.1	2.18	0.52

+LR, positive likelihood ratio; -LR, negative likelihood ratio; GSR, MRI grayscale ratio between the lesion and the surrounding normal liver parenchyma; GSRL, MRI grayscale ratio between the enhance-lesion and the plain scan-lesion; SHCC, small Hepatocellular Carcinoma; SFNH, small Focal nodular hyperplasia; AP, arterial phase; PP, portal phase; DP, delayed phase; GSRAP, GSR in the AP; GSRPP, GSR in the PP; GSRDP, GSR in the DP; GSRLAP, GSRL in the AP; GSRLPP, GSRL in the PP; GSRLDP, GSRL in the DP.

The AUCs for GSRLAP, GSRLPP, and GSRLDP in differentiating SHCC from SFNH were 0.70, 0.70, and

[DOI: 10.61186/ijrr.22.3.625]

0.78, respectively. The respective sensitivity and specificity showed to be 68.6% and 68.7%, 51.4% and 86.7%, 62.9% and 71.1%. The +LR and -LR ratio were 2.19 and 0.46, 3.86 and 0.56, 2.18 and 0.52, correspondingly. The optimal threshold values for GSRLs were 2.98, 2.89, and 2.27, and the maximum Youden indexes were 0.37, 0.38, and 0.34, respectively (figure 3, table 3).

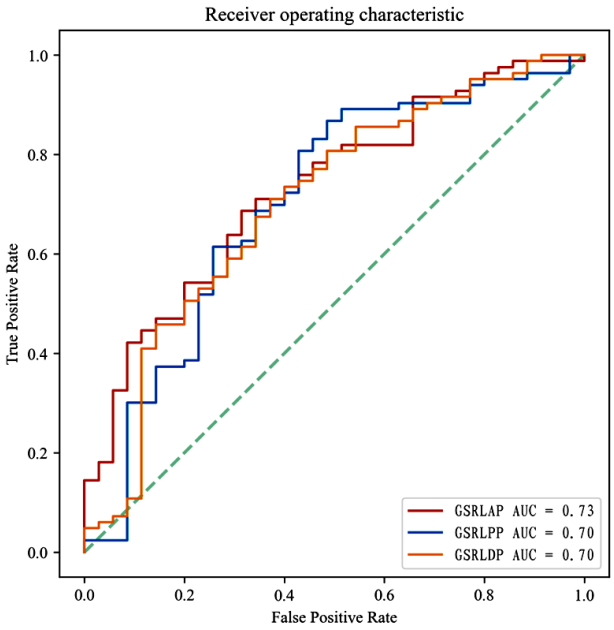

Figure 3. ROC curve generated according to GSRLAP, GSRLPP and GSRLDP values. *ROC: receiver operating curve. GSRL: MRI grayscale ratio between the enhance-lesion and the plain scan -lesion, AP: arterial phase, PP: portal phase, DP: delayed phase, GSRLAP: GSRL in the AP, GSRLPP: GSRL in the PP, GSRLDP: GSRL in the DP.*

Interobserver consistency analysis

A strong consensus was detected between the two radiologists for GSRAP (Kappa = 0.91), GSRPP (Kappa = 0.89), GSRDP (Kappa = 0.95), GSRLAP (Kappa = 0.89), GSRLPP (Kappa = 0.90), and GSRLDP (Kappa = 0.92).

DISSCUTION

In our prior research, we utilized CT-Values to differentiate between SHCC and SFNH [22]. However, in the current study, we focused on the conventional triple-enhancement MRI, leading to the following findings: 1) Statistically significant differences were observed in the GSR and GSRL values across the three enhancement phases when comparing SHCC and SFNH, with a gradual decrease. 2) In each respective phase, the parameters for SFNH were consistently higher than those for SHCC. 3) The AUC values for GSRPP and GSRDP exceeded those of GSRLPP and GSRLDP, while the AUC for GSRAP was equivalent to that of GSRLAP.

HCC exhibits a significant global incidence; however, it often remains latent in its early stages, leading to diagnosis in the intermediate or advanced stages and the potential for recurrence post-resection treatment [2,3,23]. Notably, the majority of HCC patients are elderly men, highlighting male gender as a prominent risk factor for HCC [2,3,24,25]. Conversely, patients with FNH are typically young women. The precise etiology of FNH remains unknown but could be associated with hormonal therapy and prolonged use of oral contraceptives [5,26]. While SFNH primarily affects female patients, it is interesting to note that male patients comprised 43.8% of the SFNH cohort [6,7]. This could be attributed to the fact that all SFNH patients included in this study underwent pathological confirmation.

AFP was initially introduced in the 1960s as a serological and conventional biomarker for HCC surveillance in clinical settings. However, despite setting a low-level cutoff, its diagnostic performance was suboptimal. Additionally, serum AFP levels remain within the typical range in 15-30% of advanced HCC cases [27], and nearly 30% of HCC cases in initial instances evade detection via AFP analysis [28], resulting in delays in treatment initiation. Plenty of evidence has established cirrhosis as the primary risk condition for HCC [29,30].

Real-time shear-wave elastography was harnessed to differentiate between HCC and FNH, revealing that FNH displayed greater rigidity compared to HCC [1]. Nevertheless, these distinctions could not be precisely quantified. It was reported that the contrast ratio between the lesion and the liver in HCC, exhibiting paradoxical uptake during the hepatobiliary phase, did not show any significant difference when compared to the group of nodules resembling FNH [7]. Conversely, this assessment was confined to the hepatobiliary phase, and the sample size was limited, possibly introducing some deviation.

The manifestation of washout in the portal venous and/or transitional instances was identified as the most dependable characteristic for distinguishing HCC-paradoxical from FNH-like nodules [7]. T1 mapping was employed to quantitatively assess Gd-EOB-DTPA uptake in liver focal lesions, revealing substantial variations in T1E, T1P, T1D, and T1D% between FNH and HCC, with T1D% regarded as the premier diagnostic indicator [31]. Nonetheless, specialized liver contrast agent examinations are time -intensive and expensive, rendering them unaffordable for a considerable number of patients.

The IVIM-derived extravascular effects of passive diffusion (IVIM derived D) and apparent diffusion coefficient (ADC) were suggested to be potentially adequate for distinguishing HCC from FNH (AUC showed to be 0.76 and 0.75, respectively) [18], although the sample size was low [32]. Interestingly, the effectiveness of preoperative differentiation between HCC and FNH was demonstrated by utilizing the ADC value and parameters derived from DKI,

[DOI: 10.61186/ijrr.22.3.625]

including diffusivity (D) and kurtosis (K) results [33]. Nevertheless, in comparison to our study, the diagnostic effectiveness was reduced, and DKI was not a conventional sequence.

The diagnosis of hyperintense HCC as distinct from FNH relied on features such as AP enhancement, washout patterns in active CT, and the decrease of the ADC ratio, although these could not be precisely quantified [34]. Prior investigations have shown that enhancement in the AP and PP can differentiate HCC from FNH, with the AP serving as the superior distinguishing indicator [24]. While the diagnostic accuracy of these prior studies exceeded that of the current one, they did not include DP in their comparisons, and the number of cases was limited. It is crucial to note that the potential influence of AFP and cirrhosis on the results was not taken into account in those aforementioned studies.

CONCLUSION

In this research, semi-quantitative analysis of enhanced MRI proved effective in distinguishing between SHCC and SFNH, enhancing diagnostic accuracy. Notably, among the parameters, GSRDP emerged as the most reliable indicator. The precise identification of SHCC and SFNH using these metrics has the potential to significantly minimize unwarranted intervention-related trauma.

Limitations

Nevertheless, the present work had some limitations. Variations in the physical conditions of the patients, including issues like cardiopulmonary insufficiency, may have resulted in different scanning timeframes across the three phases. Additionally, being a retrospective study, it was susceptible to selection bias. Furthermore, the investigation encompassed a relatively modest sample volume and was performed exclusively at one facility. In subsequent endeavors, our goal is to augment the sample size and undertake a multicenter exploration to enhance the generalizability of our findings. Lastly, we excluded patients with fatty liver as it could potentially cause significant fluctuations in GSV. We aim to address this challenge in future research.

ACKNOWLEDGMENTS

None.

Funding: This study was supported by the Hangzhou Agriculture and Social Development Scientific Research Guidance Project (20211231Y022), the Natural Science Foundation of Zhejiang Province (Y22H185692).

Conflict of Interest: The authors declare that they have no competing interests.

Ethical Considerations: This research was approved by the Ethics Committee of Hangzhou First People's Hospital, which is associated with Zhejiang University School of Medicine, under reference number NO. 109 - 01.

Author Contributions: XFZ: data acquisition and analysis and drafting and writing of the manuscript; QF: data analysis and data collection; XHG：important revisions to the manuscript; BH: work concept or design and important revisions to the manuscript.

REFERENCES

1. Gad MAM, Eraky TE, Omar HM, *et al.* (2021) Role of real-time shear-wave elastogarphy in differentiating hepatocellular carcinoma from other hepatic focal lesions. *Eur J Gastroenterol Hepatol,* ***33(3):*** *407-414.*
2. Tan DJH, Ng CH, Lin SY, *et al*. (2022) Clinical characteristics, surveillance, treatment allocation, and outcomes of non-alcoholic fatty liver disease-related hepatocellular carcinoma: a systematic review and meta-analysis. *Lancet Oncol,* ***23(4):*** *521-530.*
3. Hu X, Chen R, Wei Q, *et al*. (2022) The Landscape of Alpha Fetoprotein In Hepatocellular Carcinoma: Where Are We? *Int J Biol Sci,* ***18 (2):*** *536-551.*
4. Gainey CS, Palmer SL, Mena E, *et al.* (2020) Diagnosis of Focal Nodular Hyperplasia (FNH) after Liver Transplantation. *Case Rep Transplant,* ***2020:*** *8824099.*
5. LeGout JD, Bolan CW, Bowman AW, *et al*. (2022) Focal Nodular Hyperplasia and Focal Nodular Hyperplasia-like Lesions. *Radiographics,* ***42(4):*** *1043-1061.*
6. Guo Y, Li W, Cai W, *et al.* (2017) Diagnostic Value of Gadoxetic Acid -Enhanced MR Imaging to Distinguish HCA and Its Subtype from FNH: A Systematic Review. *Int J Med Sci,* ***14(7):*** *668-674.*
7. Kim JW, Lee CH, Kim SB, *et al*. (2017) Washout appearance in Gd-EOB-DTPA-enhanced MR imaging: A differentiating feature between hepatocellular carcinoma with paradoxical uptake on the hepatobiliary phase and focal nodular hyperplasia-like nodules. *J Magn Reson Imaging,* ***45(6):*** *1599-1608.*
8. Johnson P, Zhou Q, Dao DY, *et al.* (2022) Circulating biomarkers in the diagnosis and management of hepatocellular carcinoma. *Nat Rev Gastroenterol Hepatol,* ***19(10):*** *670-681.*
9. Wang T and Zhang KH (2020) New Blood Biomarkers for the Diagnosis of AFP-Negative Hepatocellular Carcinoma. *Front Oncol,* ***10:*** *1316.*
10. Affo S, Yu LX, Schwabe RF (2017) The Role of Cancer-Associated Fibroblasts and Fibrosis in Liver Cancer. *Annu Rev Pathol,* ***12:*** *153-186.*
11. Perisetti A, Goyal H, Yendala R, *et al*. (2021) Non-cirrhotic hepatocellular carcinoma in chronic viral hepatitis: Current insights and advancements. *World J Gastroenterol,* ***27(24):*** *3466-3482.*
12. Dong Y, Wang WP, Lee WJ, *et al*. (2022) Hepatocellular carcinoma in the non-cirrhotic liver. *Clin Hemorheol Microcirc,* ***80(4):*** *423-436.*
13. Singal AG, Tayob N, Mehta A, *et al*. GALAD demonstrates high sensitivity for HCC surveillance in a cohort of patients with cirrhosis. *Hepatology,* ***75(3):*** *541-549.*
14. Shavelle RM, Kwak JH, Saur R, *et al*. (2022) Life Expectancy after Liver Transplantation for Non-Cirrhotic Hepatocellular Carcinoma. *Prog Transplant,* ***31(2):*** *117-125.*
15. Usman S, Smith L, Brown N, *et al.* (2018) Diagnostic accuracy of Magnetic Resonance Imaging using liver tissue specific contrast agents and contrast enhanced Multi Detector Computed Tomography: A systematic review of diagnostic test in Hepatocellular Carcinoma (HCC). *Radiography (Lond),* ***24(4):*** *e109-e114.*
16. Wei Y, Ye Z, Yuan Y, *et al.* (2020) A New Diagnostic Criterion with Gadoxetic Acid-Enhanced MRI May Improve the Diagnostic Performance for Hepatocellular Carcinoma. *Liver Cancer,* ***9(4):*** *414-425.*
17. Chartampilas E, Rafailidis V, Georgopoulou V, *et al.* (2022) Current Imaging Diagnosis of Hepatocellular Carcinoma. *Cancers (Basel),* ***14(16):*** *3997.*
18. Klauss M, Mayer P, Maier-Hein K, *et al.* (2016) IVIM-diffusion-MRI for the differentiation of solid benign and malign hypervascular liver Lesions-Evaluation with two different MR scanners. *Eur J Radiol,* ***85(7):*** *1289-94.*
19. Chen D, Liu J, Zang L, *et al*. (2022) Integrated Machine Learning and Bioinformatic Analyses Constructed a Novel Stemness-Related

[DOI: 10.61186/ijrr.22.3.625]

Classifier to Predict Prognosis and Immunotherapy Responses for Hepatocellular Carcinoma Patients. *Int J Biol Sci,* ***18(1):*** *360-373.*
20. Vogel A, Meyer T, Sapisochin G, *et al*. (2022) Hepatocellular carcinoma. *Lance,* ***400(10360):*** *1345-1362.*
21. Wu M, Zhou RH, Xu F, *et al*. (2019) Multi-parameter ultrasound based on the logistic regression model in the differential diagnosis of hepatocellular adenoma and focal nodular hyperplasia. *World J Gastrointest Oncol,* ***11(12):*** *1193-1205.*
22. Ge X and Zhang J (2020) CT-Value (△HU and CT-Value ratio) in Differential Diagnosis of Small Hepatocellular Carcinoma from Focal Nodular Hyperplasia. *International Journal of Radiation Research,* ***18(4):*** *641-646.*
23. Kulik L, El-Serag HB (2019) Epidemiology and Management of Hepatocellular Carcinoma. *Gastroenterology,* ***156(2):*** *477-491.e1.*
24. Bröker MEE, Taimr P, de Vries M, *et al.* (2020) Performance of Contrast-Enhanced Sonography Versus MRI with a Liver-Specific Contrast Agent for Diagnosis of Hepatocellular Adenoma and Focal Nodular Hyperplasia. *AJR Am J Roentgenol,* ***214(1):*** *81-89.*
25. Lee HW and Ahn SH (2016) Prediction models of hepatocellular carcinoma development in chronic hepatitis B patients. *World J Gastroenterol,* ***22(37):*** *8314-8321.*
26. Gatti M, Calandri M, Bergamasco L, *et al*. (2020) Characterization of the arterial enhancement pattern of focal liver lesions by multiple arterial phase magnetic resonance imaging: comparison between hepatocellular carcinoma and focal nodular hyperplasia. *Radiol Med,* ***125(4):*** *348-355.*
27. Han LL, Lv Y, Guo H, *et al*. (2014) Implications of biomarkers in human hepatocellular carcinoma pathogenesis and therapy. *World J Gastroenterol,* ***20(30):*** *10249-61.*
28. Li J, Cheng ZJ, Liu Y, *et al.* (2015) Serum thioredoxin is a diagnostic marker for hepatocellular carcinoma. *Oncotarget,* ***6(11):*** *9551-63.*
29. Grandhi MS, Kim AK, Ronnekleiv-Kelly SM, *et al*. (2016) Hepatocellular carcinoma: From diagnosis to treatment. *Surg Oncol,* ***25(2):*** *74-85.*
30. Luo P, Wu S, Yu Y, *et al*. (2019) Current Status and Perspective Biomarkers in AFP Negative HCC: Towards Screening for and Diagnosing Hepatocellular Carcinoma at an Earlier Stage. *Pathol Oncol Res,* ***26(2):*** *599-603.*
31. Peng Z, Li C, Chan T, *et al.* (2017) Quantitative evaluation of Gd-EOB-DTPA uptake in focal liver lesions by using T1 mapping: differences between hepatocellular carcinoma, hepatic focal nodular hyperplasia and cavernous hemangioma. *Oncotarget,* ***8(39):*** *65435 -65444.*
32. Luo M, Zhang L, Jiang XH, *et al*. (2017) Intravoxel incoherent motion: Papplication in differentiation of hepatocellular carcinoma and focal nodular hyperplasia. *Diagn Interv Radiol,* ***23(4):*** *263-271.*
33. Jia Y, Cai H, Wang M, *et al*. (2019) Diffusion Kurtosis MR Imaging versus Conventional Diffusion-Weighted Imaging for Distinguishing Hepatocellular Carcinoma from Benign Hepatic Nodules. *Contrast Media Mol Imaging, l17; 2030147.*
34. Zarghampour M, Fouladi DF, Pandey A, *et al.* (2018) Utility of volumetric contrast-enhanced and diffusion-weighted MRI in differentiating between common primary hypervascular liver tumors. *J Magn Reson Imaging,* ***48(4):*** *1080-1090.*

[DOI: 10.61186/ijrr.22.3.625]